LA-UR -93-102

Los Alamos National Laboratory is operated by the University of California for the United States Department of Energy under contract W-7405-ENG-36.

LA-UR--93-102

DE93 007336

TITLE: USE OF R-MATRIX THEORY IN LIGHT ELEMENT EVALUATIONS

AUTHOR(S): G. M. Hale, T-2

SUBMITTED TO: The Symposium on Nuclear Data Evaluation Methodology,
Brookhaven National Laboratory, Upton, NY 12-16 October 1992

DISCLAIMER

Los Alamos National Laboratory
Los Alamos, New Mexico 87545

USE OF R-MATRIX THEORY IN LIGHT ELEMENT EVALUATIONS

G. M. HALE
Theoretical Division, Los Alamos National Laboratory
Los Alamos, New Mexico 87545, USA

ABSTRACT

R-matrix theory is a general framework for describing nuclear reactions (neutron- and charged-particle-induced) that is particularly well-suited for including resonances. We will review some unconventional properties of resonances that arise from this theory, including non-Breit-Wigner (BW) resonances and shadow poles, and discuss their physical consequences. Examples will be given from the analyses of several light systems that have been used in ENDF evaluations, including ^{4}He, ^{5}He, ^{15}N, and ^{17}O. The resonances in the helium systems tend to be significantly non-BW in character, while almost all the resonances in ^{15}N and ^{17}O are Breit-Wigner. An interesting exception in the case of ^{15}N indicates that some of the sub-threshold levels that have been assumed to be bound might be virtual. We find that fitting data from all possible reactions simultaneously results in level schemes for the compound systems that differ in some cases significantly from the "accepted" published level information.

1. Introduction

Wigner's R-matrix theory[1,2] gives an exceptionally useful description of multichannel nuclear reactions that builds in all the fundamental conservation laws, symmetries, and analytic properties (causality, unitarity, etc.) of nuclear interactions. Because it parametrizes only interior quantities, the correct Coulomb and angular-momentum barrier penetration effects are automatically built into the theory for both neutron- and charged-particle-induced reactions. Furthermore, the explicit energy dependence of the elements of the R matrix,

$$R_{c'c} = \sum_{\lambda} \frac{\gamma_{c'\lambda}\gamma_{c\lambda}}{E_\lambda - E} \tag{1}$$

as a sum of pole terms in energy, is ideally suited for describing resonances.

The resonances given by R-matrix theory for light nuclei, in particular, in terms of S-matrix pole structure sometimes have unexpected properties. The fact that S-matrix poles are in momentum, rather than energy, leads to the existence of "shadow" poles[3] on relatively remote unphysical sheets of the many-channel Riemann energy surface having positions and residues (partial widths) that can be quite different from those of the pole closest to the physical sheet that is usually identified with the resonance. In some instances, as we shall see in the case of a near-threshold resonance, shadow poles have observable effects on the measured cross sections. In other cases, the shadow poles associated with observable positive-energy resonances can become sub-threshold virtual states that previously have been thought to be bound states. Such variations in the properties of the poles on different Riemann sheets would not be expected on the basis of the Breit-Wigner (BW) approximation that is customarily used to describe resonances.

We will discuss in the next section aspects of resonances in the light compound systems ^{4}He, ^{5}He, ^{15}N, and ^{17}O. Calculations from the R-matrix analyses of all these systems have been used over at least part of the energy range in ENDF evaluations of neutron and charged-particle cross sections. Our approach in these analyses is to use data

of all types from all possible two-body reactions. The effects of a three-body breakup channel on the two-body channels of interest can be approximated by including two-body pseudo-channels, as was done in the ^{5}He analysis. The data from all reactions are then fit simultaneously with a single set of multichannel, multilevel R-matrix parameters (the reduced-width amplitudes $\gamma_{c\lambda}$ and eigenenergies E_λ from Eq. (1), and sometimes also the channel radii a_c) using the general Los Alamos R-matrix code EDA.[4] This code features an automated variable-metric least-squares fitting algorithm that allows renormalization factors and energy shifts to be applied to the measured data included in the analysis. The calculated values can also be averaged over any of several different forms of energy resolution functions.

2. Examples

2.1 The ^{5}He System

The ^{5}He system contains one of the most famous resonances in nuclear physics: the J^π=3/2$^+$ resonance responsible for the large ^{3}H(d,n)^{4}He reaction cross section that peaks at E_d=107 keV. Values of the cross section at energies below the resonance are useful in a variety of fusion applications, and at higher energies, the differential cross section is of interest as a neutron source reaction.

The channels and data included in our analysis of the ^{5}He system for excitation energies up to 21.5 MeV are summarized in Table 1. In addition to the physical two-body channels d+t and n+α, an effective n+^{4}He*(0$^+$) channel was added to represent the effects of deuteron breakup (n+p+t). More than 2600 data points from 23 different types of measurements (cross sections, polarizations, *etc.*) were described in terms of 108 free R-matrix parameters that give a minimum in chi-square space for which χ^2 per degree of freedom is 1.48. We note that a generalized phase-shift fit would require 89 real parameters to achieve the same sort of description *at a single energy*.

Table 1. Channel configuration and data summary for the ^{5}He system analysis.

Channel	l_{max}	a_c (fm)
d+t	4	5.1
n+^{4}He	4	3.0
n+^{4}He*	1	5.0

Reaction	Energy Range	# Observable Types	# Data Points	χ^2
^{3}H(d,d)^{3}H	E_d=0-8 MeV	6	704	1164
^{3}H(d,n)^{4}He	E_d=0-8 MeV	14	1121	1379
^{3}H(d,n)^{4}He*	E_d=4.8-8 MeV	1	10	26
^{4}He(n,n)^{4}He	E_n=0-28 MeV	2	793	1150
Totals:		23	2628	3719

Examples of fits to some of the integrated cross-section data are shown in Fig. 1. At the left side of the figure are shown the fits to the reaction cross section (top) and neutron total cross section (bottom) over the whole energy range of the analysis. The right side of the figure shows essentially the same data enlarged over the region of the resonance. One sees that the calculations generally represent the data within their error bars, which, particularly in the case of the LRRC'S measurements,[5] are reasonably small.

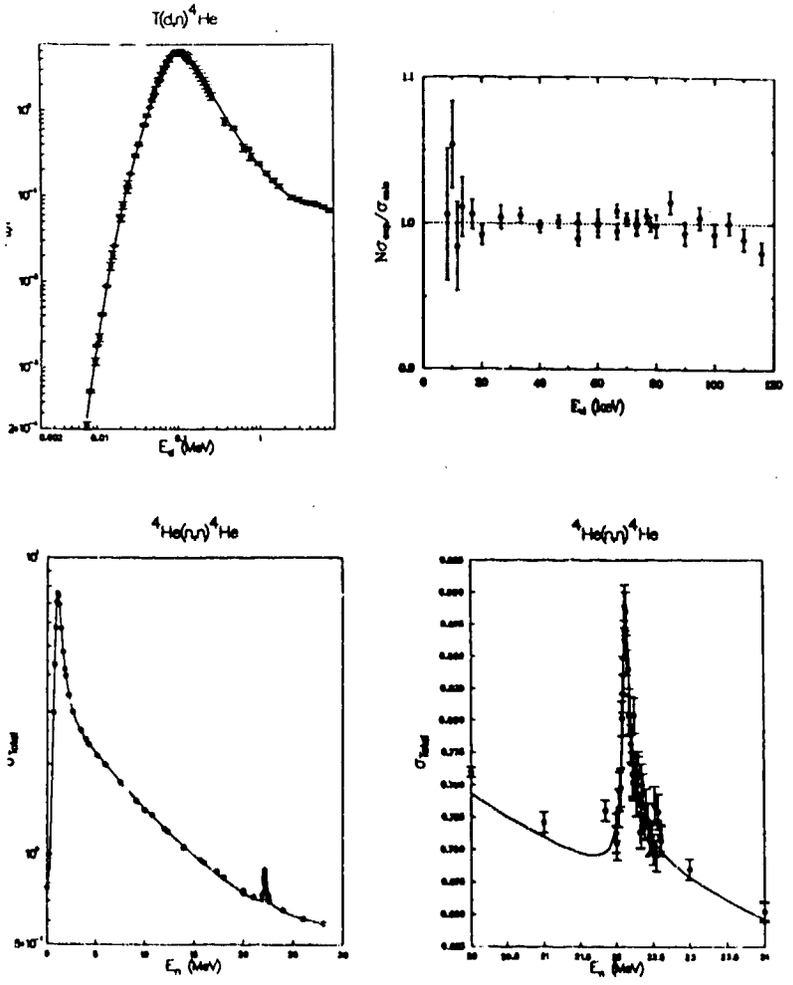

Fig. 1. ^{3}H(d,n) reaction (top) and n-α total (bottom) cross sections .

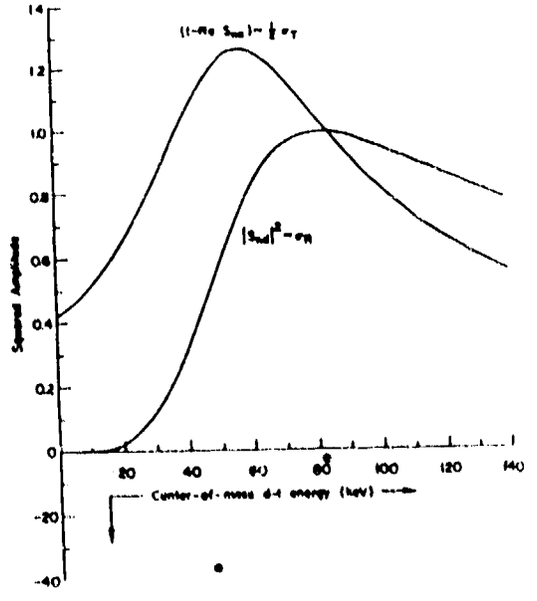

Fig. 2. ^{5}He S-matrix amplitudes over the J^π=3/2$^+$ resonance.

The energy dependence of the calculated S-matrix elements for $J^\pi=3/2^+$ that are related directly to the reaction (σ_R) and total (σ_T) cross sections are shown over the resonance in Fig. 2. Unlike the behavior that would be expected for an isolated Breit-Wigner (BW) resonance, the squared amplitudes corresponding to σ_R and σ_T do not peak at the same energy, and have a different energy dependence for the high-energy tail. Our analysis[6] shows that this behavior results from a two-pole structure of the resonance. One of the poles is a "conventional" BW pole that occurs on the (-,-)* Riemann sheet, and the other is a "shadow" pole on the (+,-) sheet. The total cross section is affected more by the conventional pole, shown as a circled "x" at the bottom left of Fig. 2, while the reaction cross section is influenced more by the shadow pole, shown by the same symbol near the real axis at 80 keV.

The resonance parameters for the poles are given in Table 2. The real and imaginary parts of the pole positions give the resonance energies E_r and total widths Γ, respectively, while the partial widths are defined in terms of the residues.[6] Note that for the conventional pole, the partial widths sum approximately to the total width, while for the shadow pole, the sum of the partials greatly exceeds the total. That is another manifestation of the non-BW character of the shadow pole, and indicates that its small value of Γ does not produce any narrow structure in the cross sections. The real reason for the lack of narrow structure associated with this pole is that one has to go around the d+t threshold in order to access the (+,-) sheet on which it lies, whereas the (-,-) sheet can be reached by dropping straight through the channel cuts along the real energy axis. The shadow pole associated with this famous resonance is the first one identified in a nuclear reaction, although a prior example was known for an elementary-particle resonance.

Table 2. Pole parameters for the ^{5}He resonance.

Sheet: (d,n)	(+,+)	(+,-)	(-,-)	(-,+)
E_r (keV)		81.57	46.97	
Γ (keV)		7.28	74.20	
Γ_d (keV)		2861.6	25.10	
Γ_n (keV)		68.77	39.83	

2.2 *The ^{4}He System*

Our R-matrix analysis of the ^{4}He system is part of a larger charge-independent (CI) analysis of all the two-body reactions in the four-nucleon (A=4) system. In this case, the $\gamma_{r\lambda}$ and E_λ in Eq. (1) for the R matrix are labeled with definite values of isospin quantum number T, with T=0 or 1. Furthermore, the reduced-width amplitudes for channels that belong to the same isospin multiplet are related by simple Clebsch-Gordan factors if their channel radii and boundary values are taken to be the same. In this way, the parameters of the (1,3) arrangement channels (p+^{3}He, n+t, p+t, and n+^{3}He) are interrelated, while those of the (2,2) arrangement (d+d, which is pure T=0) are unrelated to the others.

* The Riemann sheets are labeled by the signs of the imaginary parts of the momenta in the d+t and n+α channels, respectively.

The scheme of the CI analysis, as is shown in Fig. 3, was first to determine the T=1 parameters from an analysis of p+^{3}He scattering data at proton energies below 20 MeV. The fit gave a good representation of the 1004 data points included (χ^2 per degree of freedom is 1.23), using 47 R-matrix parameters determined at a channel radius of 4.9 fm for partial waves up through l=3. The validity of the isospin-1 parameters was then checked by comparing with the latest measurements of the n+^{3}H total cross-section and S-wave scattering lengths. All the p+^{3}He E_λ's were shifted by the internal Coulomb energy difference ΔE_C=-0.86 MeV in order to match the total cross section in the peak of a prominent P-wave resonance at E_n=3 MeV. Good agreement was found with the total cross section at all energies below 20 MeV, and with the coherent scattering length.[7]

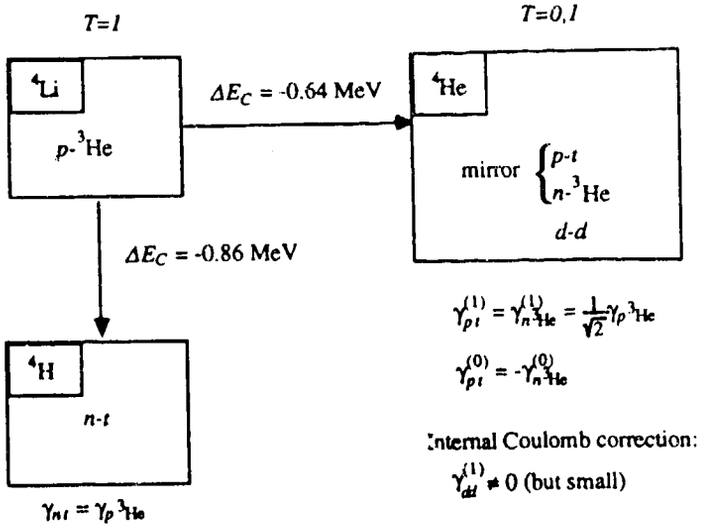

Fig. 3. Scheme of the charge-independent A=4 R-matrix analysis.

The T=1 parameters described above have been incorporated, essentially fixed, in a larger analysis of the ^{4}He reactions in which the T=0 parameters are allowed to vary. The analysis contains data from all the independent reactions among the channels p+t, n+^{3}He, and d+d at energies corresponding to ^{4}He excitations below about 29 MeV, as is summarized in Table 3. Again, an overall Coulomb energy shift allows the T=1 E_λ's to adjust to the new compound system, and the (1,3) arrangement widths are constrained by the isospin relations given in Fig. 3.

Table 3. Channel configuration and data summary for the ^{4}He system analysis

Channel	l_{max}	a_c (fm)
p+t	3	4.9
n+3He	3	4.9
d+d	3	7.0

Reaction	Energy Range	# Observable Types	# Data Points
^{3}H(p,p)^{3}H	E_p=0-11 MeV	3	1382
^{3}H(p,n)^{3}He + inv.	E_p=0-11 MeV	5	726
^{3}He(n,n)^{3}He	E_n=0-10 MeV	2	126
^{2}H(d,p)^{3}H	E_n=0-10 MeV	6	1382
^{2}H(d,n)^{3}He	E_d=0-10 MeV	6	700
^{2}H(d,d)^{2}H	E_d=0-10 MeV	6	336
Totals:		28	4652

While the fit to the 4652 data points included using 87 free parameters is not yet at a minimum of the chi-square surface (with χ^2 per degree of freedom about 4.1), the representation of the low-energy d+d reactions is quite good. The differences between the two reaction branches in the unpolarized cross sections and deuteron analyzing powers are well reproduced by allowing a small amount of internal isospin mixing to enter through the non-zero width amplitudes $\gamma_{dd}^{(T=1)}$. Although these amplitudes give widths that are less than 0.1% of the single-particle value, their effects on the P-wave transitions, in particular, are greatly amplified in the external Coulomb field by the presence of broad, overlapping negative-parity levels of opposite isospin near the d+d threshold. This is shown in Fig. 4, where the "old" level scheme[8] for ^{4}He is compared with the "new" one[9] obtained from the CI R-matrix analysis. The new T=1 levels are much lower than before, and there is a new T=0, J^π=1$^-$ level just above the d+d threshold.

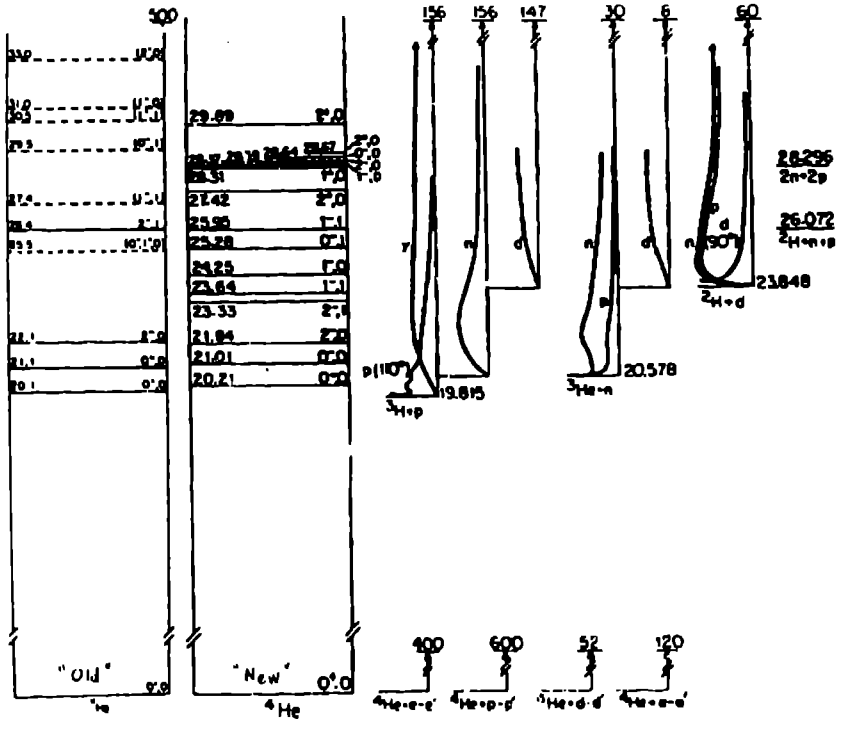

Fig. 4. Present ^{4}He level scheme (right) compared to the previous one (left).

The effects of these strongly-mixed P-wave levels can be seen most directly in branching-ratio measurements for muon-catalyzed d+d fusion at room temperature, since for identical particles, these measurements select only the P-wave part of the nuclear reaction. The experimental n/p branching ratio[10] is 1.39±0.04, but the value predicted by the analysis, 1.43±0.03, is in quite good agreement with this surprisingly large result.

2.3 *The ^{15}N and ^{17}O systems*

New R-matrix analyses were begun a few years ago for the ^{15}N and ^{17}O systems because of renewed interest in neutron transport through air in connection with a new study of radiation exposure during the Hiroshima and Nagasaki bombings. The analyses were generally limited to neutron energies below the first excited state of the target nucleus. Summaries of the channels and data included in the analyses are given in Tables 4 and 5.

Table 4. Channel configuration and data summary for ^{15}N system analysis.

Channel	l_{max}	a_c (fm)
n+^{14}N	2	2.5
p+^{14}C	3	4.3
α+^{11}B	2	5.1

Reaction	Energy Range	Observable Types	# Data Points
^{14}N(n,n)^{14}N	E_n=0-2.4 MeV	σ_T, $\sigma_{nn}(\theta)$	932
^{14}N(n,p)^{14}C + inv.	E_n=0-2.4 MeV	σ_{np}, $\sigma_{pn}(\theta)$, $A_p(\theta)$	685
^{14}N(n,α)^{11}B	E_n=1.3-2.4 MeV	$\sigma_{n\alpha}$	104
^{11}B(α,p)^{14}C	E_α=1.4-2.6 MeV	$\sigma_{\alpha p}$, $\sigma_{\alpha p}(\theta)$	110
Totals:		8 obs.	1831

The calculated n+^{14}N total cross sections are shown compared to the recent ORELA measurements[11] in Fig. 5. The agreement is now quite good over the whole range of the analysis, which was not the case when the measurements were first made. This was particularly true of the first resonance at E_n=433 keV, for which the previous measurements had been severely resolution-limited, and did not allow the true J-value (7/2) to be inferred from the peak cross section. We have assigned a positive parity for this resonance, in agreement with preliminary angular distribution measurements also made at ORELA. Other J^π assignments are indicated on the figure, some of which differ from the "accepted" level structure[12] tabulated for ^{15}N, but correspond to resonances that have largely Breit-Wigner characteristics.

Table 5. Channel configuration and data summary for the ^{17}O system analysis.

Channel	l_{max}	a_c (fm)
n+^{16}O	4	4.4
α+^{13}C	4	5.7

Reaction	Energy Range	Observable Types	# Data Points
^{16}O(n,n)^{16}O	E_n=0-6.5 MeV	σ_T, $\sigma_{nn}(\theta)$, $A_n(\theta)$	2421
^{16}O(n,α)^{13}C	E_n=0-6.0 MeV	$\sigma_{n\alpha}$, $\sigma_{n\alpha}(\theta)$, $A_n(\theta)$	904
^{13}C(α,α)^{13}C	E_α=0-4.6 MeV	$\sigma_{\alpha\alpha}(\theta)$	207
Totals:		7 obs.	3532

Calculated n+^{16}O cross sections are shown in Fig. 6 compared to measured data. Again, the agreement is good over the entire energy range of the analysis, and the J^π values indicated on the resonances do not always agree with the "accepted" values.[13] Most of the resonances again have BW character, with shadow poles in about the same positions on all unphysical sheets, having partial widths that sum to the total width. An interesting exception is a shadow pole associated with the lowest-energy 1/2$^-$ resonance at E_n=1.9 MeV that is a virtual state located very close to the energy of the second excited state (1/2$^-$) in ^{17}O. This sub-threshold state is a prediction of the analysis, based on fitting only the scattering data.

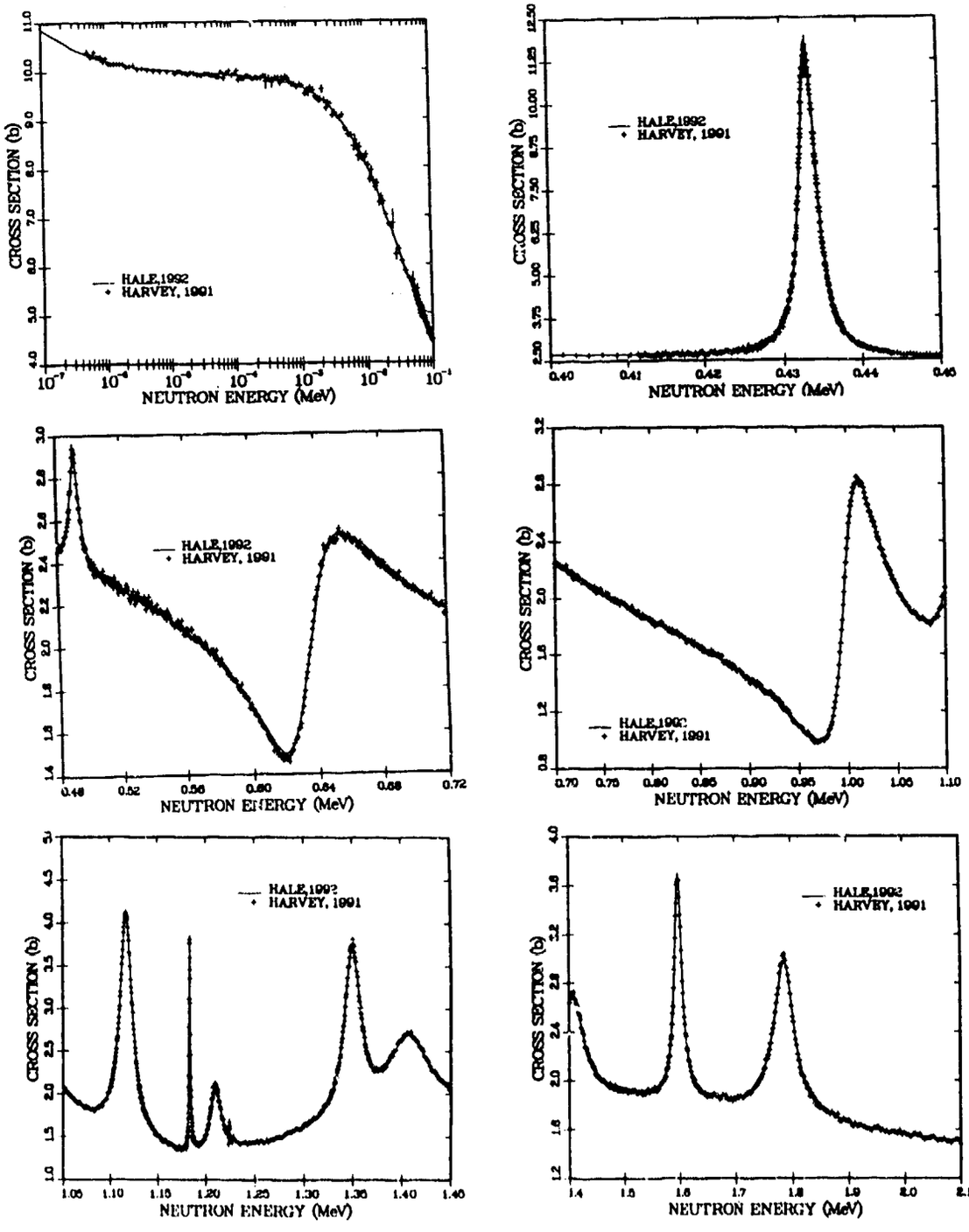

Fig. 5 Calculated n+^{14}N total cross sections compared to the data of Harvey[11] at energies below 2.1 MeV.

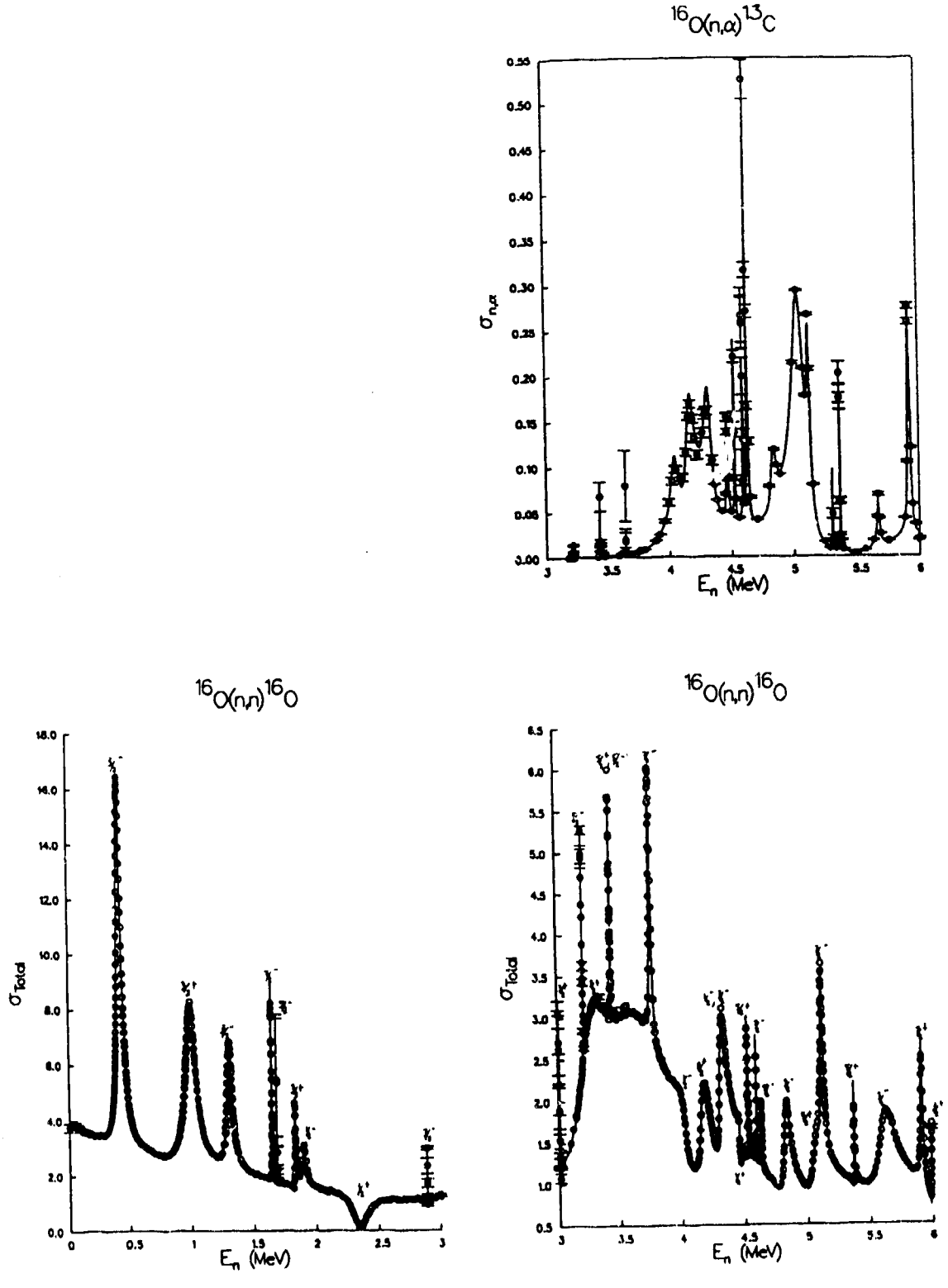

Fig. 6. Neutron total (bottom) and (n,α) reaction cross sections for neutrons on ^{16}O.

3. Summary and Conclusions

We have given several examples of using *R*-matrix theory to fit data for the light systems. Our experience has convinced us that there is no better method for representing data for multichannel systems, especially if resonances are present. It is important, however, to include data of many types from all possible reactions in order to reduce the possibility of parameter ambiguities in the chi-square fitting, and to insure the reliability of extrapolated results.

R-matrix theory predicts that all multichannel nuclear resonances have shadow poles that, in principle, have different properties on different Riemann sheets, contrary to the expectations of BW resonance forms. As a practical matter, these differences occur mainly for the broad resonances in very light nuclei, and appear to be important only near thresholds, where several unphysical sheets are nearly equally accessible from the physical sheet. The first example of an observable shadow pole in a nuclear reaction is the famous $J^{\pi}=3/2^{+}$ resonance in the ^{5}He system, where the presence of the pole on the (+,-) sheet near the real energy axis drives the reaction amplitude almost to its unitary limit, resulting in the large ^{3}H(d,n)^{4}He reaction cross section observed at low energies. Shadow poles also play a role in other ^{4}He and ^{5}He resonances, especially in producing threshold effects.

The charge-independent analysis of the A=4 reactions illustrates the utility of being able to constrain *R*-matrix parameters with approximate symmetries of the strong interactions. In this case, strong isospin mixing of *P*-wave levels near the d+d threshold that comes rather naturally from the description is able to account for the anomalous branching ratios seen in d+d muon-catalyzed fusion experiments. Other ^{4}He levels that result from the analysis do not agree with the previous scheme, but correspond well with those from a microscopic resonating-group-model calculation of the system.

The resonances resulting from analyzing the heavier ^{15}N and ^{17}O systems tend more often to satisfy the BW conditions, although they differ in detail with the "accepted" level structures for these nuclei. An interesting result for ^{17}O is the virtual state that occurs as a "shadow" to the 1/2^{-} scattering resonance some 3 MeV higher in excitation energy. This suggests that more examples of virtual states like the well-known "singlet deuteron" may exist among the sub-threshold levels of light nuclei now thought to be bound states.

4. References

1. E. P. Wigner and L. Eisenbud, *Phys. Rev.* **72** (1947) 29.
2. A. M. Lane and R. G. Thomas, *Rev. Mod. Phys.* **30** (1958) 257.
3. R. J. Eden and J. R. Taylor, *Phys. Rev.* **133** (1964) B1575.
4. D. C. Dodder, G. M. Hale, and K. Witte, "Energy Dependent Analysis Code for Nuclear Reactions," Los Alamos National Laboratory (unpublished).
5. N. Jarmie, R. E. Brown, and R. A. Hardekopf, *Phys. Rev. C* **29** (1984) 2031; R. E. Brown, N. Jarmie, and G. M. Hale, *Phys. Rev. C* **35** (1987) 1999.
6. G. M. Hale, R. E. Brown, and N. Jarmie, *Phys. Rev. Lett.* **59** (1987) 763.
7. G. M. Hale, D. C. Dodder, J. D. Seagrave, B. L. Berman, and T. W. Phillips, *Phys. Rev. C* **42** (1990) 438.
8. S. Fiarman and W.E. Meyerhof, *Nucl. Phys.* **A206** (1973) 1.
9. D. R. Tilley, H. R. Weller, and G. M. Hale, *Nucl. Phys.* **A541** (1992) 1.
10. D. V. Balin et al., *Phys. Lett.* **141B** (1984) 173; *JETP Lett.* **40** (1984) 112.
11. J. A. Harvey, N. W. Hill, N. M. Larson, and D. C. Larson, in *Nuclear Data for Science and Technology*, ed. S. M. Qaim (Springer-Verlag, Berlin, 1992) 729.
12. F. Ajzenberg-Selove, *Nucl. Phys.* **A523** (1991) 1.
13. F. Ajzenberg-Selove, *Nucl. Phys.* **A460** (1986) 1.